

Measurement of the astrophysical S factor for the low energy ${}^2\text{H}(\text{d},\gamma){}^4\text{He}$ reaction

ZHOU Jing(周静)¹⁾ FU Yuan-Yong(傅元勇) ZHOU Shu-Hua(周书华)
XIA Hai-Hong(夏海鸿) LI Cheng-Bo(李成波) MENG Qiu-Ying(孟秋英)

(China Institute of Atomic Energy, Beijing 102413, China)

Abstract The γ -rays and protons from an $E_d = 20$ keV deuteron beam incident on a D—Ti target were measured. A branching ratio of the ${}^2\text{H}(\text{d},\gamma){}^4\text{He}$ reaction versus the ${}^2\text{H}(\text{d},\text{p}){}^3\text{H}$ reaction of $\Gamma_\gamma/\Gamma_p = (1.06 \pm 0.34) \times 10^{-7}$ has been obtained, and the astrophysical S factor of the ${}^2\text{H}(\text{d},\gamma){}^4\text{He}$ reaction at the center of mass energy $E_{\text{cm}} \approx 7$ keV of $(6.0 \pm 2.4) \times 10^{-6}$ keV·b was deduced.

Key words ${}^2\text{H}(\text{d},\gamma){}^4\text{He}$ reaction, branching ratio, S factor

PACS 25.45.-z, 26.20.Np, 25.40.Lw

1 Introduction

In the energy range of 10—100 keV, the ${}^2\text{H}(\text{d},\gamma){}^4\text{He}$ reaction is of fundamental importance for the determination of deuteron burning and the ${}^4\text{He}$ abundance in astro-nuclear processes^[1]. Besides this, the cross section of this reaction below 100 keV is crucial in ascertaining the temperature of deuterium–deuterium plasma^[2, 3] and in evaluating the production of heat in cold fusion experiments^[4]. Investigation of the ${}^2\text{H}(\text{d},\gamma){}^4\text{He}$ reaction can provide significant information for the understanding of the reaction mechanism among light charged particles and the ground state structure of α particles^[5–9]. So the study of the ${}^2\text{H}(\text{d},\gamma){}^4\text{He}$ reaction has been an interesting topic since the first measurement by Zurmühle and Stephens^[10].

The ${}^2\text{H}(\text{d},\gamma){}^4\text{He}$ reaction is involved in both primordial and stellar nucleosynthesis^[7, 11, 12]. The observation that the astrophysical S factor, $S(E_{\text{cm}}) = \sigma(E_{\text{cm}})E_{\text{cm}} \exp(2\pi\eta)$, where η is the Sommerfeld parameter, decreases steeply with decreasing energy and that the angular distributions^[5, 10, 13] are of the form $\sin^2\theta \cos^2\theta$ for $E_{\text{cm}} \geq 0.4$ MeV confirms that the reaction mainly proceeds via an E2 transition from the 1D_2 component in the entrance channel to the 1S_0 component of the ${}^4\text{He}$ ground state. However, later

work^[7] has indicated that at $E_{\text{cm}} < 80$ keV the $S(E)$ factor clearly deviates from the trend at high energies and suggested an initial 5S_2 state, which could lead to a determination of the ${}^4\text{He}$ D -state admixture, as well as a 32 times higher $S(0)$ value than previously adopted for astrophysical work^[11]. Although it has been pointed out that the ${}^2\text{H}(\text{d},\gamma){}^4\text{He}$ rate does not change the previously drawn conclusions from standard big bang nucleosynthesis models^[14], the altered $S(0)$ value may be significant in inhomogeneous big bang nucleosynthesis models with regions of high neutron density^[15]. In the present work, we extended the measurement of the branching ratio of the ${}^2\text{H}(\text{d},\gamma){}^4\text{He}$ reactions versus the ${}^2\text{H}(\text{d},\text{p}){}^3\text{H}$ reactions to a deuteron beam energy of 20 keV, and deduced the astrophysical S factor down to an effective center of mass energy of 7 keV.

2 Experiment

The experimental arrangement and some preliminary results have been briefly reported in Ref. [16]. A deuteron beam of 20 keV was produced by the low-energy acceleration facility (LEAF) at the China Institute of Atomic Energy. This facility is composed of a microwave ion source, a solenoidal lens, an analyzing magnet and acceleration and deceleration sec-

Received 3 June 2008

1) E-mail: jzh@ciae.ac.cn

©2009 Chinese Physical Society and the Institute of High Energy Physics of the Chinese Academy of Sciences and the Institute of Modern Physics of the Chinese Academy of Sciences and IOP Publishing Ltd

tions. The deuterium-loaded titanium targets on Mo backings were about 0.5 mg/cm^2 thick. The atomic ratio of deuterium to tritium was 1.7:1. The beam intensity was about 5–8 mA and the size of the beam spot on the target was $10\text{ mm}\times 20\text{ mm}$. Circulating cold water was used to cool the target. A sketch of the experimental arrangement is shown in Fig. 1. The γ -rays were detected with a $20\text{ cm}\times 20\text{ cm}$ NaI(Tl) detector, which was surrounded by a 10 cm thick plastic scintillator detector with another 10 cm thick plastic scintillator detector in front as an anti-coincidence shield for rejecting the cosmic ray background. Outside of the surrounding plastic scintillator, a shield composed of 10 cm of lead and 38 cm of lithium carbonated paraffin was used to reduce the background γ -rays and neutrons. By carefully adjusting the electronics, 96% of the cosmic ray background detected by the NaI(Tl) detector was rejected in the 20–25 MeV energy range (see Fig. 2). The axis of the γ -ray detector assembly was at 8.5° to the beam. The protons produced from the ${}^2\text{H}(d,p){}^3\text{H}$ reactions were detected with a $\phi 8$ GM type Au-Si surface barrier semiconductor detector placed at the end of a 100 cm long tube, which was perpendicular to the beam line. There were two anti-scattering diaphragms to prevent the scattered protons from hitting the detector and a 3.03 mm collimator to define the solid angle. The proton detector was covered with aluminum foil $2\text{ }\mu\text{m}$ in thickness to stop the scattered protons and other charged particles. Energy calibration of the γ -ray detector was made using 0.662 MeV γ -rays of ${}^{137}\text{Cs}$, 1.33 MeV γ -rays of ${}^{60}\text{Co}$ and 6.13 MeV γ -rays from a Pu-C neutron source. Energy calibration of the proton detector was made using 5.24 MeV α particles of a ${}^{239}\text{Pu}$ source. The signals of the NaI(Tl) detector were sent to a multichannel pulse-height analyzer

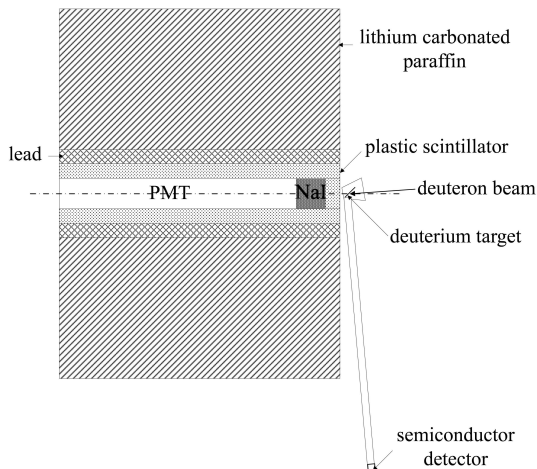


Fig. 1. Experimental arrangement.

gated by the anti-coincidence signals from the plastic scintillators. Simultaneously, the charged particle signals from the semiconductor detector were analyzed by another multichannel pulse-height analyzer.

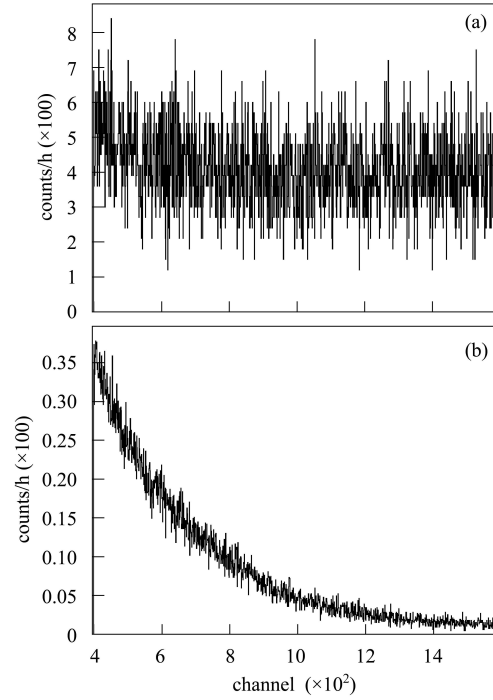


Fig. 2. Cosmic ray background spectra from the γ -ray channel without (a) and with (b) anti-coincidences.

The γ -ray detection efficiency of the NaI(Tl) detector in the shield was simulated with the MCNP code. In the simulation an isotropic angular distribution of the γ -rays was assumed, because at low energies such as 75 keV and below, $E2$ transition from a 5S_2 scattering state to the 5D_0 component of the ${}^4\text{He}$ ground state becomes the dominant mode^[7]. Since the main process of the interactions is pair production and the Compton scattering cross section is one order of magnitude smaller than that for pair production for the γ -rays of 23.8 MeV, the efficiency was integrated from 22.6 MeV to 24.0 MeV in the simulation. Thus, the full energy, single escape and double escape peaks were all included. The simulated efficiency is 7.5×10^{-2} with an estimated uncertainty of $\pm 20\%$. The proton detection efficiency was determined by the solid angle and the angular distribution of the protons, which was adopted from the differential cross section of the ${}^2\text{H}(d,p){}^3\text{H}$ reaction at $E_d = 19.944\text{ keV}$ from Ref. [17].

The measurements were performed over 126 h with the beam on and over 1024 h with the beam off to measure the radiation background, which is mainly composed of the remaining cosmic ray background, and was fitted with a function of $\exp(P_0 + P_1x + P_2x^2)$.

Fig. 3(a) shows the raw spectra of the γ -ray channel both with beam on and beam off. One can see that there is a peak near channel 145 in the beam-on spectrum. Fig. 3(b) shows the same spectrum with the fitted beam-off spectrum subtracted. However, some background still exists, mostly due to neutron-induced reactions. This background was fitted with a function of $P_0+P_1x+P_2x^2+P_3 \exp(-0.5 \times ((x-P_4)/P_5)^2)$ and subtracted from the spectrum in Fig. 3(b). Then a clean γ -ray peak shows up in Fig. 3(c). This peak corresponds to 23.8 MeV according to the calibration.

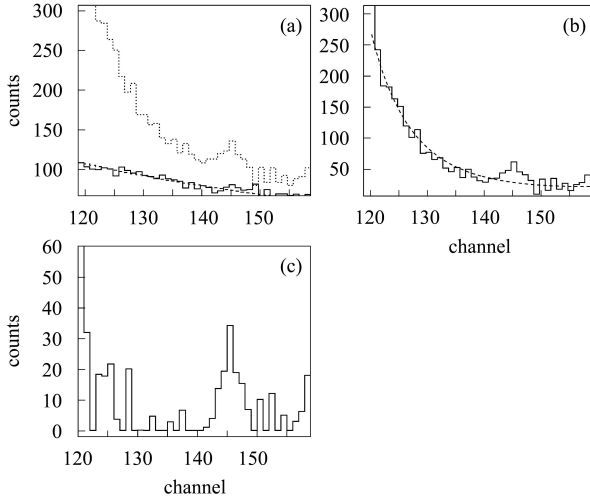


Fig. 3. (a) The γ -ray spectrum with $E_d(\text{lab}) = 20$ keV beam-on (dotted) and beam-off spectrum (solid) with fit (dashed line), (b) the same spectrum as (a) but with the fitted beam-off spectrum subtracted, and neutron-induced background with fit (dashed line), (c) the γ -ray spectrum with neutron background subtracted from (b). Near channel 145 is the 23.8 MeV γ -ray peak.

Figure 4 shows a typical proton spectrum (in one run) from the ${}^2\text{H}(d,p){}^3\text{H}$ reaction.

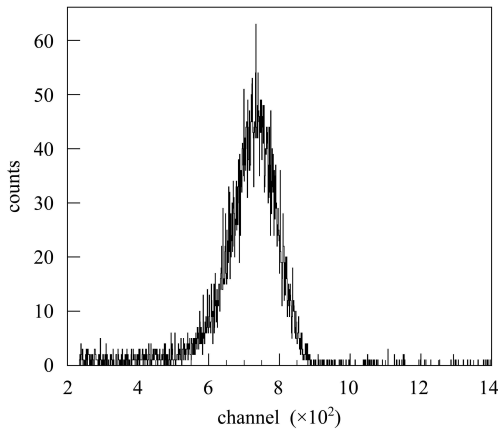


Fig. 4. A typical proton spectrum from the ${}^2\text{H}(d,p){}^3\text{H}$ reaction at $E_d(\text{lab}) = 20$ keV.

3 Results

By integrating the simultaneously measured 23.8 MeV γ -ray peak and proton peak, the ratio Y_γ/Y_p can be obtained.

The detected γ -ray yield per incident deuteron of energy E_0 is expressed by

$$Y_\gamma = \varepsilon_\gamma(E_\gamma) \int_{E_0}^0 \frac{\Gamma_\gamma}{\Gamma_{\text{tot}}} \frac{\sigma_{\text{tot}}(E)}{\frac{dE(E)}{dn}} f(E) dE. \quad (1)$$

Similarly, the proton yield is

$$Y_p = \varepsilon_p(E_p) \int_{E_0}^0 \frac{\Gamma_p}{\Gamma_{\text{tot}}} \frac{\sigma_{\text{tot}}(E)}{\frac{dE(E)}{dn}} f(E) dE. \quad (2)$$

In the above two equations $\varepsilon_\gamma(E_\gamma)$ and $\varepsilon_p(E_p)$ are the detection efficiencies, $\Gamma_\gamma/\Gamma_{\text{tot}}$ and $\Gamma_p/\Gamma_{\text{tot}}$ are the γ to total and proton to total branching ratios, respectively, $\sigma_{\text{tot}}(E)$ is the total cross section for the D+D reaction, $dE(E)/dn$ is the stopping power, and $f(E)$ is the fractional density of deuterium atoms in the target at an incident deuteron energy depth. Assuming that $\Gamma_\gamma/\Gamma_{\text{tot}}$ and $\Gamma_p/\Gamma_{\text{tot}}$ are independent of energy^[6], then the ratio Γ_γ/Γ_p is related to the yield of the γ -rays and that of the protons as follows:

$$\frac{\Gamma_\gamma}{\Gamma_p} = \frac{Y_\gamma \varepsilon_p(E_p)}{Y_p \varepsilon_\gamma(E_\gamma)}. \quad (3)$$

By integrating the net γ -ray peak area, we obtained the number of detected γ -rays to be 208. After the efficiency correction we have $Y_\gamma/\varepsilon_\gamma(E_\gamma) = (1.60 \pm 0.49) \times 10^4$. Similarly, we have $Y_p/\varepsilon_p = (1.51 \pm 0.12) \times 10^{11}$. In the calculation of ε_p , we used the angular distribution data from Ref. [17]. Then from equation (3) the branching ratio is calculated to be $\Gamma_\gamma/\Gamma_p = (1.06 \pm 0.34) \times 10^{-7}$. The error mainly comes from the efficiency calculation of the γ -ray detector and the particle detector. Fig. 5 shows the measured Γ_γ/Γ_p ratios from the present work (solid circle) and from Refs. [4, 6]. It should be pointed out, that the energy loss calculation shows that the 20 keV incident deuterons will stop in the 0.5 mg/cm² thick D—Ti target, and the center of mass energy E_{cm} lies in fact in the range of 10 to 0 keV. According to the theoretical calculation^[18] of the energy dependence of the cross sections, the average cross section is equal to the cross section at $E_{\text{cm}} = 7$ keV. So, the branching ratio Γ_γ/Γ_p , which we measured in the experiment, corresponds to the effective center of mass energy of ~ 7 keV.

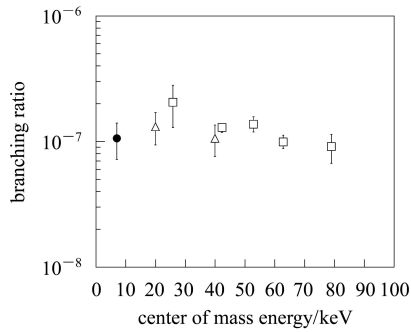


Fig. 5. The Γ_γ/Γ_p ratios in the $E_{\text{cm}}(\text{D-D}) = 7\text{--}80$ keV energy range. The solid circle is from the present work, open triangles are from Ref. [4] and open squares are from Ref. [6].

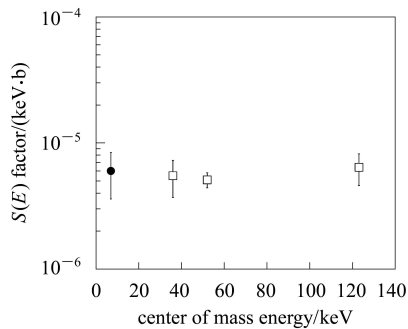


Fig. 6. The $S(E)$ factor of ${}^2\text{H}(d,\gamma){}^4\text{He}$ reactions. The solid circle is from the present work, the open squares are from Ref. [7].

To deduce the S factor of the ${}^2\text{H}(d,\gamma){}^4\text{He}$ reaction by using a linear least-squares fit, we extrapolated the S factor of the ${}^2\text{H}(d,p){}^3\text{H}$ reaction^[17] to 7 keV. Then using the Γ_γ/Γ_p branching ratio from the present experiment we derived the astrophysical S factor of the ${}^2\text{H}(d,\gamma){}^4\text{He}$ reaction at the center of mass energy ~ 7 keV to be $S = (6.0 \pm 2.4) \times 10^{-6}$ keV·b. This value is comparable with Barnes' results at the

effective center of mass energy 36 keV $((5.5 \pm 1.8) \times 10^{-6}$ keV·b), 52 keV $((5.1 \pm 0.7) \times 10^{-6}$ keV·b) and 123 keV $(6.4 \pm 1.8) \times 10^{-6}$ keV·b^[7] (see Fig. 6). By linear Extrapolation of the S values from the three lowest energies in Fig. 6, we obtained $S(0) = 6.2 \pm 2.5 \times 10^{-6}$ keV·b.

4 Conclusion

We extended the measurement of the branching ratio for the ${}^2\text{H}(d,\gamma){}^4\text{He}$ reaction versus the ${}^2\text{H}(d,p){}^3\text{H}$ reaction to 20 keV deuteron beam energy. The present result $\Gamma_\gamma/\Gamma_p = (1.06 \pm 0.34) \times 10^{-7}$, together with the earlier work^[4, 6], shows that below a center of mass energy of 80 keV the branching ratio is roughly constant. This behavior can not be explained by a purely electric quadrupole capture ($E2$) process. An admixture of magnetic dipole capture might exist (see Fig. 5 in Ref. [6]). The branching ratio at very low energies can be used in estimating whether significant heat production is possible from cold (D-D) fusion reactions in the absence of enormous quantities of escaping hazardous. We also extracted the astrophysical S factor for the ${}^2\text{H}(d,\gamma){}^4\text{He}$ reaction at the effective center of mass energy ~ 7 keV. Compared with earlier results^[7], the present result means that from $E_{\text{cm}} = 123$ keV to 7 keV the S value is almost energy independent, and that the extrapolated $S(0)$ value should be about 30 times larger than that estimated previously^[11].

We thank Jiang Weisheng and Cui Baoqun for useful discussions, and acknowledge Jiang Chong for providing the deuteron beam for the experiment.

References

- 1 Foeler W A. Rev. Mod. Phys., 1984, **56**: 149
- 2 Medlty S S, Hendel H. Bull. Am. Phys. Soc., 1982, **26**: 980
- 3 Newman D E. Nucl. Instrum. Methods, 1984, **221**: 49
- 4 Cecil F E, Hale G M. The Science of Cold Fusion Como. Italy: Societa Italiana di Fisica, Bologna, Italy, 1991
- 5 Meyerhof Walter E et al. Nucl. Phys. A, 1969, **131**: 489
- 6 Wilkinson F J, Cecil F E. Phys. Rev. C, 1985, **31**: 2036
- 7 Barnes C A et al. Phys. Lett. B, 1987, **197**: 315
- 8 Langenbrunner J L et al. Phys. Rev. C, 1990, **42**: 1214
- 9 Kramer L H et al. Phys. Lett B, 1993, **304**: 208
- 10 Zurmühle R W, Stephens W E. Phys. Rev., 1963, **132**: 751
- 11 Fowler W A, Caughlan G R, Zimmerman B A. Annu. Rev. Astron. Astrophys., 1967, **5**: 525
- 12 Arnett W D, Truran J W. Nucleosynthesis-Challenges and New Developments. Chicago: University of Chicago Press, 1985
- 13 Poutissou J M, Bianco W D. Nucl. Phys. A, 1973 **199**: 517
- 14 Santos F D, Yun J Lin. J. Phys. G: Nucl. Part. Phys., 1989, **15**: 1275
- 15 App J H, Hogan C J, Scherrer R J. Phys. Rev. D, 1987, **35**: 1151
- 16 ZHOU Shu-Hua et al. Chin. Phys. Lett., 2006, **23**: 2703
- 17 Brown Ronald E, Jarmie Nelson. Phys. Rev. C, 1990, **41**: 1391
- 18 MA Yin-Qun, MA Zhong-Yu, TIAN Yuan. HEP & NP, 2006, **30**: 1242 (in Chinese)